

1 **Exonuclease III (XthA) enforces *in vivo* DNA cloning of *Escherichia coli* to create**
2 **cohesive ends**

3

4 Shingo Nozaki¹ and Hironori Niki^{1,2}

5

6 ¹Microbial Physiology Laboratory, Department of Gene Function and Phenomics,
7 National Institute of Genetics, 1111, Yata, Mishima, Shizuoka, Japan 411-8540

8

9 ²Department of Genetics, the Graduate University for Advanced Studies (SOKENDAI),
10 1111, Yata, Mishima, Shizuoka, Japan 411-8540

11

12 Corresponding author: Hironori Niki

13 hniki@nig.ac.jp

14 055-981-6870

15 Microbial Physiology Laboratory, Department of Gene Function and Phenomics,
16 National Institute of Genetics, 1111, Yata, Mishima, Shizuoka, Japan 411-854

17

18 **Abstract**

19 *Escherichia coli* has an ability to assemble DNA fragments with homologous
20 overlapping sequences of 15-40 bp at each end. Several modified protocols have already
21 been reported to improve this simple and useful DNA-cloning technology. However, the
22 molecular mechanism by which *E. coli* accomplishes such cloning is still unknown. In
23 this study, we provide evidence that the *in vivo* cloning of *E. coli* is independent of both
24 RecA and RecET recombinase, but is dependent on XthA, a 3' to 5' exonuclease. Here,
25 *in vivo* cloning of *E. coli* by XthA is referred to as iVEC (*in vivo E. coli* cloning). Next,
26 we show that the iVEC activity is reduced by deletion of the C-terminal domain of
27 DNA polymerase I (PolA). Collectively, these results suggest the following mechanism
28 of iVEC. First, XthA resects the 3' ends of linear DNA fragments that are introduced
29 into *E. coli* cells, resulting in exposure of the single-stranded 5' overhangs. Then, the
30 complementary single-stranded DNA ends hybridize each other, and gaps are filled by
31 DNA polymerase I. Elucidation of the iVEC mechanism at the molecular level would
32 further advance the development of *in vivo* DNA-cloning technology. Already we have
33 successfully demonstrated multiple-fragment assembly of up to seven fragments in
34 combination with an effortless transformation procedure using a modified host strain for
35 iVEC.

36

37 **Importance**

38 Cloning of a DNA fragment into a vector is one of the fundamental techniques in
39 recombinant DNA technology. Recently, *in vitro* recombination of DNA fragments
40 effectively joins multiple DNA fragments in place of the canonical method.

41 Interestingly, *E. coli* can take up linear double-stranded vectors, insert DNA fragments
42 and assemble them *in vivo*. The *in vivo* cloning have realized a high level of usability
43 comparable to that by *in vitro* recombination reaction, since now it is only necessary to
44 introduce PCR products into *E. coli* for the *in vivo* cloning. However, the mechanism of
45 *in vivo* cloning is highly controversial. Here we clarified the fundamental mechanism
46 underlying *in vivo* cloning of *E. coli* and also constructed an *E. coli* strain that was
47 optimized for *in vivo* cloning.
48

49 **Introduction**

50 Cloning of a DNA fragment into a vector is one of the fundamental techniques in
51 recombinant DNA technology. As the standard procedure for DNA cloning, a method
52 using restriction enzymes and DNA ligases has long been used. Recently, modified
53 methods of DNA cloning have been widely adopted in place of the canonical method.
54 For example, for the joining of DNA fragments to vectors, an *in vitro* recombination
55 reaction is used. In particular, enzymatic assembly of DNA fragments by using T5
56 exonuclease, DNA polymerase and DNA ligase effectively joins multiple DNA
57 fragments (1). T5 exonuclease resects the 5' ends of the terminal overlapping sequences
58 of the DNA fragments to create the 3' ends of single-stranded DNA overhangs. The
59 complementary single-stranded DNA overhangs are annealed, the gaps are filled, and
60 the nicks are sealed enzymatically. A similar reaction also occurs with the crude cell
61 extract of *Escherichia coli* (2, 3).

62 In contrast to DNA cloning utilizing *in vitro* recombination, some strains of *E.*
63 *coli* can take up linear double-stranded vectors, insert DNA fragments and assemble
64 them *in vivo* (4, 5). The ends of these linear DNA fragments need to share 20-50 bp of
65 overlapping sequences with homology. DNA amplification by PCR readily provides
66 this type of linear DNA fragment of interest. Following its introduction, in the early
67 1990s, this simpler cloning method was not widely used. Recently, however, it has been
68 brought to scientific attention and has been improved with various strains of *E. coli* and
69 several PCR-based protocols (6-12). These improved protocols for *in vivo* cloning have
70 realized a high level of usability comparable to that by *in vitro* recombination reaction,
71 since now it is only necessary to introduce PCR products into *E. coli* for the *in vivo*
72 cloning.

73 The mechanism of *in vivo* cloning is highly controversial. Initially, the
74 *sbcA23* mutant of the *E. coli* strain JC8679 was used for *in vivo* cloning because the
75 expression of RecE exonuclease and RecT recombinase, here referred to as RecET
76 recombinase, of λ prophage is activated in this mutation (5, 13). Then, it was thought
77 that a recombination pathway of the prophage was involved in the *in vivo* cloning.
78 However, *E. coli* strains without *sbcA23* mutation, such as DH5 α , also have the
79 sufficient ability for *in vivo* cloning (4, 8, 9). Recently, it was suggested that the ability
80 for *in vivo* cloning is not limited to specific mutant strains (10, 11). If *in vivo* cloning is
81 not dependent on host *E. coli* strains, then the DNA substrates may be responsible for
82 the *in vivo* cloning. Klock *et al.* considered that the DNA fragments prepared by PCR
83 have a single-stranded DNA region resulting from incomplete primer extension, and
84 hybridization between complementary single-stranded ends promotes the pathway for *in*
85 *vivo* cloning (6). On the other hand, Li *et al.* conjectured that 3' to 5' exonuclease
86 activity of high-fidelity DNA polymerase creates a single-stranded region at the ends of
87 the linear DNA fragments during PCR (7). Thus, the DNA fragments with single-
88 stranded overhangs produced by PCR seem to be a key for *in vivo* cloning. However,
89 the linear DNA fragments prepared with a restriction enzyme that generates blunt ends
90 are also capable of *in vivo* cloning, indicating that other mechanisms such as a gap
91 repair reaction should be considered (8). In general, the mechanism of *in vivo* cloning
92 remains unclear.

93 Here we clarified the mechanism underlying the *in vivo* cloning of *E. coli* and
94 also constructed an *E. coli* strain that was optimized for *in vivo* cloning. In addition, we
95 streamlined the procedure of *in vivo* cloning by introducing a newly developed
96 transformation procedure using a single microcentrifuge tube.

97 Results

98 The iVEC activity in various strains

99 To identify the principle mechanism underlying the *in vivo* cloning in *E. coli*, here
100 referred to as iVEC, we first confirmed the iVEC activity in various conventionally
101 used strains of *E. coli*. We performed a simple assay of the iVEC activity by
102 transforming the strains with two DNA fragments that carry 20 bp of homologous
103 overlaps at their ends: a *cat* gene encoding chloramphenicol acetyltransferase and the
104 vector plasmid pUC19 (**Fig. 1A**). As a result, transformants resistant to both ampicillin
105 and chloramphenicol appeared in all of the strains tested, although the efficiency of
106 transformation varied depending on the host cells (**Fig. 1B**). MG1655 and JC8679, in
107 particular, had fewer transformants than the other strains. In order to confirm that the
108 *cat* gene was cloned into pUC19, purified plasmids derived from the transformants were
109 analyzed. All of the purified plasmids were larger than the empty vector, pUC19 (**Fig.**
110 **1C**). When the plasmids were digested with *Bam*HI, a single band was detected in each
111 lane and the length of the band matched that of the cloned plasmid (**Fig. 1D**). Insertion
112 of DNA into the vector was also confirmed by PCR (**Fig. 1E**).

113 Due to the smaller number of positive colonies in MG1655 and JC8679, we
114 noticed that these strains have the wild-type *hsdR* gene. The three other strains, DH5 α ,
115 AG1 and BW25113, have a mutation in *hsdR*. HsdR is a host specificity restriction
116 enzyme, which degrades DNA containing an unmethylated Hsd recognition sequence
117 (14), and pUC19 DNA contains the recognition sequence. Therefore, we introduced a
118 deletion mutation of the *hsdR* gene into MG1655 and JC8679, resulting in SN1054 and
119 SN1071, respectively. As a result, the numbers of ampicillin- and chloramphenicol-
120 resistant colonies after introduction of both the *cat* fragment and linearized pUC19 were

121 significantly increased by the deletion of *hsdR* (**Fig. 1F**). Thus, various *E. coli* strains
122 essentially have the capacity to recombine short homologous sequences at the ends of
123 linear DNAs, permitting the *in vivo* cloning of DNA fragments into linearized vectors.
124

125 ***recA* and *recET* are dispensable for the iVEC activity**

126 To elucidate the mechanism of iVEC activity in MG1655, we tested whether
127 recombination proteins such as RecA or RecET were required for the *in vivo* cloning
128 ability. For this purpose, we introduced deletion mutations of the *recA* or *recET* genes
129 into SN1054. We then examined the iVEC activity by transforming these deletion
130 mutants with the *cat* fragment and linearized pUC19. As a result, we found that deletion
131 of *recA* or *recET* had little effect on iVEC activity (**Fig. 2A**), indicating that RecA and
132 RecET are dispensable for *in vivo* cloning.

133

134 ***xthA* is required for the iVEC activity**

135 In general, DNA recombination in *E. coli* accompanies conversion of double-stranded
136 DNA to single-stranded DNA by exonuclease. It is reported that *E. coli* has at least
137 seven exonucleases that prefer double-stranded DNA for their substrates as follows:
138 XthA, RecE, ExoX, RecBCD, SbcCD, Nfo and TatD (15). In addition, YgdG is an
139 exonuclease whose preferential substrate is unknown. Next, therefore, we examined the
140 iVEC activity in deletion mutants of these exonucleases. We used the deletion mutants
141 from the Keio collection because BW25113, the parental strain of the Keio collection,
142 has sufficient capacity for iVEC, as shown in Fig. 1B.

143 We tested each deletion mutant by introducing a DNA fragment containing
144 the *cat* gene and linearized pUC19 vector. As a result, in the $\Delta xthA$ mutant, the iVEC

145 activity was remarkably decreased to 0.7% of that in the wild-type strain (**Fig. 2B**). The
146 iVEC activity was slightly decreased in the $\Delta exoX$, $\Delta recB$, $\Delta recC$, Δnfo and $\Delta tatD$
147 mutants. However, because these defects were several orders of magnitude smaller than
148 that observed in the $\Delta xthA$ mutant, we focused on XthA in the subsequent experiments.

149 There was a possibility that deficiency in plasmid maintenance or DNA
150 uptake was the reason for the remarkable reduction of iVEC activity in the $\Delta xthA$
151 mutant. Therefore, we examined the level of transformation efficiency of the $\Delta xthA$
152 mutant by using circular DNA of the pUC19 plasmid and found that it was almost
153 equivalent to the efficiency of the $xthA^+$ strain (**Fig. 2C**). This indicates that plasmid
154 maintenance and DNA uptake are normal in the $\Delta xthA$ strain. Since XthA (exonuclease
155 III) has 3' to 5' exonuclease activity (16), we speculated that resection of the DNA ends
156 by this enzyme to produce single-stranded overhangs is crucial for iVEC activity. To
157 confirm this idea, we introduced DNA fragments in which 20 bp of the single-stranded
158 overhangs at the ends were generated in advance, into the $\Delta xthA$ mutant (**Fig. 2D**). As a
159 result, in the $\Delta xthA$ mutant, a sufficient number of transformants comparable to the
160 number in the $xthA^+$ strain were obtained from the DNA fragments with overhangs,
161 whereas DNA fragments with blunt ends yielded few recombinants (**Fig. 2E**).
162 Hybridizing between homologous single-stranded DNA regions of the introduced DNA
163 fragments regardless of 5' or 3' overhangs would be essential for recombination of the
164 DNA fragments in the host cell. We concluded that the exonuclease activity of XthA to
165 produce single-stranded overhangs plays a critical role in iVEC activity.

166 Although XthA is a major factor for the iVEC activity, a small number of
167 recombinant plasmids were still produced in the $\Delta xthA$ mutant (**Fig. 2F**). The
168 transformants were obtained even when a mutation of $\Delta recA$ or $\Delta recET$ was added to

169 the $\Delta xthA$ mutant. We confirmed that the recombinant plasmids were correctly
170 assembled even in the $\Delta xthA$ mutant (**Fig. 2G and 2H**). Thus, faint iVEC activity still
171 remained in the $\Delta xthA$ mutant. These results suggest that there are other minor
172 pathway(s) for iVEC activity, which are independent of XthA, RecA and RecET.

173

174 ***polA* affects the iVEC activity**

175 Our results suggested that, following the production of single-stranded DNA segments
176 by XthA, homologous single-stranded DNA segments are hybridized and gaps are
177 produced. We considered that specific DNA polymerases fill the gaps to ligate the
178 hybridized DNA fragments To address which DNA polymerase is involved in gap
179 filling, we examined the effect of defects in DNA polymerases on the iVEC activity. *E.*
180 *coli* has five DNA polymerases (17). Among them, Pol II, Pol IV and Pol V encoded by
181 *polB*, *dinB* and *umuCD*, respectively, are non-essential for cell growth. Therefore, first,
182 we tested the iVEC activities in the deletion mutants of non-essential DNA
183 polymerases. All of these deletion mutants—i.e., $\Delta polB$, $\Delta dinB$ $\Delta umuC$ and $\Delta umuD$ —
184 showed little effect on the iVEC activity (**Fig. 3A**). Thus, these polymerases are not
185 involved in the iVEC activity.

186 Next, we examined the requirement of DNA polymerase I (Pol I) for the
187 iVEC activity. Pol I and Pol III are essential for cell growth. Pol III is a core enzyme of
188 the DNA polymerase III holoenzyme, which is the primary enzyme complex involved
189 in prokaryotic DNA replication. Hence, we considered that it would be difficult to
190 analyze the iVEC activity by using a mutant of pol III. On the other hand, although the
191 *polA* gene encoding Pol I is essential, the full length of this gene is not required for cell
192 viability (18). Only the N-terminal domain encoding 5' to 3' exonuclease is sufficient

193 for cell growth (19). Indeed, a *polA1* mutant which expresses only 341 amino acid
194 residues at the N-terminus of PolA by the amber mutation at the amino acid residue 342
195 is viable (20) (**Fig. 3B**). Accordingly, we constructed a mutant strain carrying the *polA1*
196 mutation, along with deletion of a part of the *polA* gene that encodes the C-terminal 587
197 amino acid residues including the DNA polymerase domain. The resulting *polA1ΔC*
198 mutant expresses the N-terminal 341 amino acid residues in the manner of the *polA1*
199 mutant. Since the full-length PolA is required for the initiation step of pUC19
200 replication, we used pMW119 to assay iVEC activity (**Fig. 3C**). The replication origin
201 of pMW119 is derived from pSC101, which does not require the *polA* product for the
202 initiation of its replication (21). The transformation efficiencies of the *polA1ΔC* and the
203 $\Delta xthA$ mutant with pMW119 were similar to that of a wild-type strain, SN1054 (**Fig.**
204 **3D**). We measured the iVEC activity of SN1054 and the $\Delta xthA$ and *polA1ΔC* mutants
205 by simultaneous introduction of linearized pMW119 and a DNA fragment containing
206 the *cat* gene with a 20 bp overlapping sequence at the ends. High iVEC activity was
207 observed by using pMW119 in the wild-type strain but not in the $\Delta xthA$ mutant (**Fig.**
208 **3E**). Thus, *xthA* played a critical role in the iVEC activity when a pSC101-derivative
209 plasmid vector was used. This result certainly suggests that application of iVEC is not
210 limited to pUC-derivative plasmids. The number of transformants of the *polA1ΔC*
211 mutant decreased to about one third of that of the wild-type strain, and this difference
212 was statistically significant ($p = 0.00037$ by Welch's T test). In conclusion, the C-
213 terminal domain of PolA was not fully responsible for, but did partly contribute to the
214 iVEC activity.

215

216 **Optimization of a host strain for iVEC**

217 Since strains derived from MG1655 had the highest iVEC activity, we attempted to
218 optimize the host strain based on MG1655. Many *E. coli* strains used for DNA
219 manipulation, including DH5 α , harbor a mutation in the *endA* gene, which encodes a
220 DNA-specific endonuclease I (22), to improve the quantity of recovered plasmids.
221 Therefore, we introduced a deletion mutation of the *endA* gene into the *E. coli* strain
222 MG1655, along with a deletion mutation of the *hsdR* gene. The number of positive
223 colonies for iVEC increased by two-fold in $\Delta endA$ cells compared with that of the
224 *endA*⁺ strain (**Fig. 4A**). We examined the transformation efficiency of the $\Delta endA$ strain
225 with pUC19 plasmid DNA and found that it was increased (**Fig. 4B**). This result
226 indicates that the improvement of the iVEC activity in the $\Delta endA$ strain was caused by
227 increased transformation efficiency due to the DNA stability during the DNA uptake
228 process.

229 In *E. coli*, dimer plasmid DNA is accumulated due to homologous
230 recombination (23). To prevent the dimerization of recombinant plasmids, we
231 introduced a *recA* deletion mutation into a host strain carrying the $\Delta hsdR \Delta endA$ strain,
232 resulting in SN1187. Although *recA* deletion mutation often causes lower
233 transformation efficiency due to a reduction in cell viability, the iVEC activity and
234 transformation efficiency of SN1187 were not deteriorated by the deletion mutation of
235 *recA* (**Fig. 4A, B**). Moreover, the amount of dimer was drastically decreased when
236 plasmid DNA was retrieved from SN1187 and analyzed by using agarose gel
237 electrophoresis (**Fig. 4C**).

238

239 **Multiple fragment cloning by the host strain SN1187**

240 We further evaluated a new host strain, SN1187, in terms of its capacity for iVEC.

241 First, we examined whether certain lengths of homologous sequences at the ends of
242 DNA fragments were required. We tested DNA fragments with overlapping sequences
243 of 15 bp to 30 bp in length (**Fig. 5A**). In this experiment, the numbers of ampicillin-
244 resistant colonies after introduction of both linearized pUC19 and the *cat* fragment were
245 counted. Approximately 600, 1000, 3200 and 3700 ampicillin-resistant colonies
246 appeared when we used DNA fragments with overlapping sequences of 15 bp, 20 bp, 25
247 bp and 30 bp at their ends, respectively (**Fig. 5B**). Most of the colonies (99% to 100%)
248 were also resistant to chloramphenicol, indicating that the DNAs were correctly
249 assembled in those colonies (**Fig. 5C**). On the other hand, when only linearized pUC19
250 was introduced, only 5 ampicillin-resistant transformants appeared (**Fig. 5B**). This result
251 suggests that carryover of a small amount of template vector from PCR yielded few
252 undesirable transformants, despite the fact that *DpnI* digestion of the template DNA
253 from PCR was not carried out.

254 We also examined whether iVEC with SN1187 is available for multi-
255 fragment assembly. First, we introduced three DNA fragments (linearized pUC19 and
256 the DNA fragments including the *cat* or *kan* gene) with 20 bp overlapping sequences at
257 their ends (**Fig. 5D**). Also in this experiment, we selected transformants with only
258 ampicillin resistance, which is a marker of vector DNA, for practical purposes. As a
259 result, about 200 ampicillin-resistant colonies were obtained (**Fig. 5E**). When we
260 examined whether 96 randomly selected, ampicillin-resistant colonies were also
261 resistant to chloramphenicol and kanamycin, we found that all 96 colonies were
262 resistant to chloramphenicol and kanamycin as well as ampicillin (**Fig. 5F**). Next, the
263 assembly of four fragments (linearized pUC19 and the DNA fragments including the
264 *cat*, *kan*, or *tet* gene) was carried out with 20 to 40 bp of homologous overlapping

265 sequences (**Fig. 5D**). We obtained about 20, 60, 90 and 180 ampicillin-resistant colonies
266 with homologous overlaps of 20, 25, 30 and 40 bp, respectively (**Fig. 5E**). The ratios of
267 colonies resistant to all of ampicillin, chloramphenicol, kanamycin and tetracycline
268 against colonies resistant to ampicillin alone ranged from 80% to 95% (**Fig. 5F**). We
269 also read joint sequences of assembled DNAs to confirm the accuracy of recombination.
270 When 8 plasmids per each construct of two, three and four fragments assembly with 20
271 bp overlapping sequences were examined, no base change was found within
272 overlapping sequences (**Fig. S1A, S1B, S1C**). Finally, we attempted to perform
273 simultaneous gene assembly of seven fragments. Each of the DNA fragments used for
274 the assembly of four fragments was split and assembled with 40 bp homologous
275 overlaps at its ends (**Fig. 5D**). About 40 colonies resistant to ampicillin were obtained
276 (**Fig. 5E**). Among those ampicillin-resistant colonies, about 60% were also resistant to
277 each of the antibiotics chloramphenicol, kanamycin and tetracycline (**Fig. 5F**). This
278 result indicated that the DNA fragments that included antibiotic-resistance genes
279 separated into 6 fragments were correctly assembled at the same time. We also
280 examined joint sequences of this recombinant plasmid. For this purpose, plasmid DNA
281 from 8 independent colonies was examined. While one plasmid had a 2 bp region of
282 deletion within a joint segment, no base change was found in the other plasmids (**Fig.**
283 **S1D**). Finally, we demonstrated that purification of the PCR products was not necessary
284 for the iVEC activity. When unpurified PCR products were used directly for iVEC
285 without PCR purification, the number of positive colonies was more than 500 (**Fig. 5G,**
286 **5H**). The PCR products can be used easily and relatively quickly without the
287 requirement of any treatments such as column purification, ethanol precipitation or
288 *DpnI* digestion before transformation.

289 **Discussion**

290 XthA, also known as exodeoxyribonuclease III, XthA is exodeoxyribonuclease III,
291 exhibits 3'-5' exonuclease activity. Introducing DNA fragments with cohesive ends into
292 the *E. coli* cells effectively bypasses the requirement of XthA for the iVEC activity
293 (**Fig. 2E**). On the other hand, addition of cohesive ends to insert and vector DNA
294 fragments also strengthens the iVEC activity in wild-type cells (**Fig. 2E**). This is
295 consistent with the previous reports that generation of cohesive ends during PCR is
296 effective for *in vivo* cloning (6, 7). Taken together, these facts indicate that the creation
297 of cohesive ends from the blunt ends of DNA fragments is crucial for the *in vivo*
298 cloning. Therefore, we conclude that XthA exonuclease converts the blunt ends of
299 double-stranded DNA to 5'-protruding ends in the process of the *in vivo* cloning. In
300 consideration of this activity, we propose the following as the most likely mechanism
301 for iVEC as shown in Fig. 6. After the insert and the vector DNA fragments are
302 introduced into the *E. coli* cell, XthA resects the ends of the DNA fragments from the 3'
303 to 5' direction, producing 5' overhanging ends. As the ends of insert and vector DNAs
304 have mutually complementary sequences, the 5' overhanging ends of the insert and the
305 vector DNA fragments hybridize to each other as cohesive ends. In addition, the gaps
306 are filled by DNA polymerases and the nicks are repaired by DNA ligases. Deletion of
307 the DNA polymerase domain of PolA did not completely abrogate the iVEC activity
308 (**Fig. 3E**). There is a redundant polymerase(s) for the gap filling in iVEC. It is possible
309 that pol II, III, IV or V is involved in the gap filling in the *polA1ΔC* background.

310 Previously, a strain in which the expression of RecET recombinase was
311 activated by the *sbcA23* mutation was used as a host strain for the *in vivo* cloning (5).
312 Therefore, it was thought that RecET was the recombinase essential for the *in vivo*

313 cloning. While strains without *sbcA23* mutation have been shown to possess the iVEC
314 activity (4, 8, 9), it was not clear whether even a low level expression of RecET was
315 sufficient for iVEC. The present finding that the $\Delta recET$ mutant exhibited sufficient
316 iVEC activity indicates that RecET is not required for iVEC (**Fig. 2A**). In addition, *E.*
317 *coli* has other exonucleases in addition to XthA, but their contribution to the iVEC
318 activity is relatively low (**Fig. 2B**). Interestingly, $\Delta xthA$ cells still maintained slight
319 iVEC activity that was independent of *recA* or *recET* (**Fig. 2F**). This residual activity
320 was not due to PCR-based production of single-stranded overhangs, since it was
321 observed even in the assembly of DNA fragments with blunt ends (**Fig. 2E**). It thus
322 seems likely that some other exonucleases are responsible for the residual iVEC activity
323 in $\Delta xthA$ cells. XthA would be the dominant exonuclease that preferentially digests
324 double-stranded DNA to produce single-stranded overhangs. Under most conditions, an
325 *E. coli* strain having the exonuclease activity of XthA would be able to assemble DNA
326 fragments with blunt ends that are generated by using a conventional PCR.

327 Several derivatives of *E. coli* K-12 showed the activity of iVEC, suggesting
328 that no specific mutations are required for the iVEC activity. It seems likely that *E. coli*
329 K-12 originally acquired the iVEC activity, and the iVEC activity was involved in an
330 unknown physiological function in *E. coli*. It is conceivable that XthA would help to
331 repair minor DNA damage, instead of the RecBCD exonuclease. RecBCD produces a 3'
332 overhang and loads RecA onto the single-stranded DNA, causing an SOS response
333 accompanied by cell division arrest (24). To help avoid such a serious outcome, it
334 is conceivable that XthA could function in a repair pathway of DNA damage.

335 In our present experiments, we found that the wild-type strain of *E. coli*
336 exhibits iVEC activity, although in general this activity is not high in wild-type strains.

337 To improve the efficiency of iVEC, deletion mutations of *hsdR* and *endA* are
338 introduced. The *hsdR* gene encodes a Type I restriction enzyme, *EcoKI* (25), and *EndA*
339 is a non-specific DNA endonuclease (22). Both gene disruptions improve the
340 transformation efficiency of the DNA fragments rather than the assembly process. It
341 was expected that enhancement of the expression of *xthA* by using a *T5/lac* promoter
342 would improve the iVEC activity. However, we found that the enhanced expression did
343 not increase the iVEC activity.

344 We used a modified-TSS method to measure iVEC activity. Cells in overnight
345 culture were used to prepare competent cells for the measurement. Overnight-standing
346 culture allows the entire process to be performed using only a single microcentrifuge
347 tube, from the preparation of competent cells to transformation. In this way, competent
348 cells of many different strains can be easily prepared. However, the transformation of
349 plasmid DNA is not very high: about $10^4 - 10^5$ CFU/ μ g pUC19 (**Fig. 4B**). Therefore, by
350 using less than 10-100 pg of template plasmids in PCR products, the background of
351 unwanted vector-only colonies can be significantly reduced. This also means that *DpnI*
352 treatment after PCR of vector DNA is dispensable in order to reduced transformants by
353 the template plasmid DNA. In fact, we could almost surely obtain the desired colonies
354 despite a lower number of transformants. The number of positive transformants
355 obtained with iVEC using our method and the host strain, SN1187, is comparable or
356 greater than that in previous reports using other methods such as the rubidium chloride
357 method or commercially available competent cells.

358 Obviously, *E. coli* cells can simultaneously uptake multiple DNA fragments
359 via an unknown mechanism. As a result, assembly of up to seven fragments was
360 possible by using iVEC (**Fig. 5D, 5E, 5F**). In addition, this approach was effective for

361 obtaining recombinant products of less than 10 Kbp in total. To hybridize the cohesive
362 ends of DNA fragments, shorter DNA fragments would be suitable because the
363 opportunity for initial contact between the ends of the DNA fragments increases. At
364 present, our procedure could be utilized for multi-site-directed mutagenesis instead of
365 primer extension mutagenesis. Unexpectedly, single-stranded DNA binding protein
366 (SSB) seemed not to predominantly affect the single-stranded DNA segment that was
367 exposed by XthA. It is conceivable that there is a mechanism to avoid the interference
368 by SSB and promote hybridization between cohesive ends. An improved understanding
369 of the iVEC activity would contribute to the development of iVEC methods in the
370 future.

371 **Methods**

372 **Medium**

373 L broth (1% Difco tryptone, 0.5% Difco yeast extract, 0.5% NaCl, pH adjusted to 7.0
374 with 5N NaOH) was used for liquid culture. The agar plate was made of L broth and
375 1.5% agar. The following antibiotics were used as needed: 50 µg/mL of ampicillin, 10
376 µg/mL of chloramphenicol, 15 µg/mL of kanamycin and 10 µg/mL of tetracycline.

377

378 **Bacterial strains and plasmids**

379 *E. coli* strains and plasmids used in this work are listed in **Table S1 and S2**,
380 respectively. To construct a $\Delta hsdR::frt$ mutant, a chromosomal DNA segment
381 containing $\Delta hsdR::kan$ was amplified from genomic DNA of the $\Delta hsdR::kan$ strain in
382 the Keio collection by PCR using the primer set [hsdR_F and hsdR_R] (26). The
383 amplified DNA fragments were introduced into the parent strains with pKD46 as
384 described by Datsenko and Wanner (27). The $\Delta xthA::kan$, $\Delta recET::kan$ and
385 $polA1\Delta C::kan$ strains were constructed in a similar manner using the primer sets and
386 templates [xthA_F, xthA_R and chromosome of Keio $\Delta xthA::kan$], [recET_F, recET_R
387 and pKD4] and [polAdelC_F, polAdelC_R and pKD4], respectively. The *kan* cassette
388 was removed by pCP20, if needed (27). To construct a $\Delta recA$ strain, a plasmid DNA of
389 pKH5002SB was amplified by using the primer set [pKH_F and pKH_R]. Upstream
390 and downstream chromosomal segments of the *recA* gene were amplified from MG1655
391 genomic DNA by using the primer sets [recAup_F and recAup_R] and [recAdown_F
392 and recAdown_R]. We obtained a 1.8 kb upstream chromosomal segment and a 2 kb
393 downstream chromosomal segment of *recA*, respectively. Both the recAup_F primer
394 and the recAdown_R primer have an additional 20 bp complementary sequence

395 complementary to primers pKH_R and pKH_F, respectively. In addition, 40 bp of a
396 sequence within the primers recAup_R and recAdown_F are complementary to each
397 other. Amplified DNA fragments of pKH5002SB, the upstream and the downstream
398 regions of chromosomal segment of *recA* were introduced into a $\Delta rnhA::kan$ strain to
399 generate pKH5002SB $\Delta recA$ (**Fig. S2A**). Using this plasmid, the *recA* gene was deleted
400 with two successive homologous recombinations as described previously (28) (**Fig.**
401 **S2B**). The $\Delta hsdR$ and $\Delta endA$ strains were constructed by using the same method with
402 the primer sets [hsdRup_F, hsdRup_R, hsdRdown_F and hsdRdown_R] and
403 [endAup_F, endAup_R, endAdown_F and endAdown_R], respectively.

404

405 **Preparation of PCR products for transformation**

406 We used KOD plus Neo (TOYOBO) for PCR. The thermal cycler program was as
407 follows: 94 °C for 2 min, followed by 30 cycles of [98 °C for 10 sec, 58 °C for 10 sec,
408 and 68 °C for 30 sec/kb], and a final extension of 68 °C for 5 min. Oligonucleotide
409 primers used for PCR are listed in **Table S3** and **S4**. The final concentration of the
410 template DNA in each reaction mixture was adjusted to 1 pg/ μ L, e.g., 50 pg in a 50 μ L
411 reaction. The *cat* (chloramphenicol-resistance) and *tet* (tetracycline-resistance) genes
412 were amplified from pACYC184 DNA, and the *kan* (kanamycin-resistance) gene was
413 amplified from pACYC177 DNA. All PCR products were purified using a Wizard SV
414 PCR Clean-Up System (Promega). Digestion of template DNA by *DpnI* was not
415 necessary after PCR.

416

417 **Preparation of DNA fragments with blunt ends, 5' overhangs or 3' overhangs**

418 DNA fragments with blunt ends, 5' overhangs or 3' overhangs were prepared as follows.

419 To isolate single-stranded strands, we used a Long ssDNA Preparation kit
420 (BioDynamics Laboratory, Tokyo). Plasmids used for the isolation of ssDNAs are
421 listed in **Table S2**. Each pair of the top and the bottom single-stranded DNA fragments
422 for blunt ends, 5' overhangs or 3' overhangs was mixed and incubated at 99 °C for 5
423 minutes and annealed at 65 °C for 30 minutes to generate double-stranded DNA.

424

425 **Transformation**

426 To introduce DNA fragments into *E. coli* cells, we used the TSS method with
427 modification (29). A small number of cells in a colony on an agar plate was picked up
428 using a sterilized toothpick and suspended in a 1.5 mL microcentrifuge tube containing
429 1 mL of L broth. The tube lid was closed. The tube was standing in an incubator at 37
430 °C for 20 hours without shaking. After standing incubation for 20 hours, the OD₆₀₀ of
431 the culture reached approximately 1.4 and the number of cells in the tube was about 4 x
432 10⁸ CFU/mL. The tube was chilled on ice for 10 minutes and centrifuged at 5,000 g for
433 1 minute at 4 °C to spin down the cells. The supernatant was removed, and the cell
434 pellet was dissolved in 100 µL of ice-cold TSS solution (50% L broth, 40% 2xTSS
435 solution and 10% DMSO) mixed with DNA. The composition of 2xTSS solution was
436 [20% (w/v) PEG8000, 100 mM MgSO₄ and 20% (v/v) glycerol in L broth]. For DNA
437 cloning, 0.05 pmol of linearized vector and 0.15 pmol of each insert DNA fragment
438 were used. After gentle mixing, the solution was immediately frozen in liquid nitrogen
439 for 1 minute. Frozen tubes were transferred to an ice bath. After 10 minutes of
440 incubation on ice, the tubes were briefly vortexed to mix their contents and incubated on
441 ice for an additional 10 minutes. Then, 1 mL of L broth was added, and the contents of
442 the tube were mixed by inversion and incubated at 37 °C for 45 minutes. After

443 incubation, the cells were centrifuged and the supernatant was roughly discarded. The
444 cell pellet was dissolved in the remaining supernatant and the cell suspension was
445 spread on an L agar plate containing appropriate antibiotics. Finally, the plates were
446 incubated at 37 °C for 16 hours and the number of colonies was counted. To examine
447 transformation efficiency, 1 ng of the indicated circular plasmids was used.

448

449 **Assay of the iVEC activity**

450 DNA fragment containing an antibiotic-resistance gene and linearized pUC19 with 20
451 bp homologous overlapping ends were amplified by PCR and introduced into *E. coli*
452 cells by modified-TSS method as described above (**Fig. 1A**). In a standard assay of the
453 iVEC activity, 0.15 pmol of *cat* fragment and 0.05 pmol of linearized pUC19 were used
454 for transformation of indicated strains. We counted number of colonies resistant to both
455 ampicillin and chloramphenicol after simultaneous introduction of *cat* fragment and
456 linearized pUC19 into indicated strains.

457 **Acknowledgements**

458 We thank Dr. Katsuhiko Hanada for the critical suggestions on *in vivo* cloning. We
459 thank NBRP *E. coli* for providing *E. coli* strains and plasmids. This work was supported
460 by a JSPS KAKENHI Grant (no. 8K19193).

461 **References**

- 462 1. **Gibson DG, Young L, Chuang R-Y, Venter JC, Hutchison CA, Smith HO.** 2009.
463 Enzymatic assembly of DNA molecules up to several hundred kilobases. *Nat Methods*
464 **6**:343–345.
- 465 2. **Zhang Y, Werling U, Edelmann W.** 2012. SLiCE: a novel bacterial cell extract-based
466 DNA cloning method. *Nucleic Acids Res* **40**:e55.
- 467 3. **Motohashi K.** 2015. A simple and efficient seamless DNA cloning method using SLiCE
468 from *Escherichia coli* laboratory strains and its application to SLiP site-directed
469 mutagenesis. *BMC Biotechnol* **15**:47.
- 470 4. **Bubeck P, Winkler M, Bautsch W.** 1993. Rapid cloning by homologous recombination
471 in vivo. *Nucleic Acids Res* **21**:3601–3602.
- 472 5. **Oliner JD, Kinzler KW, Vogelstein B.** 1993. In vivo cloning of PCR products in *E.*
473 *coli*. *Nucleic Acids Res* **21**:5192–5197.
- 474 6. **Klock HE, Koesema EJ, Knuth MW, Lesley SA.** 2008. Combining the polymerase
475 incomplete primer extension method for cloning and mutagenesis with microscreening to
476 accelerate structural genomics efforts. *Proteins* **71**:982–994.
- 477 7. **Li C, Wen A, Shen B, Lu J, Huang Y, Chang Y.** 2011. FastCloning: a highly
478 simplified, purification-free, sequence- and ligation-independent PCR cloning method.
479 *BMC Biotechnol* **11**:92.
- 480 8. **Jacobus AP, Gross J.** 2015. Optimal cloning of PCR fragments by homologous
481 recombination in *Escherichia coli*. *PLoS ONE* **10**:e0119221.
- 482 9. **Kostylev M, Otwell AE, Richardson RE, Suzuki Y.** 2015. Cloning Should Be Simple:
483 *Escherichia coli* DH5 α -Mediated Assembly of Multiple DNA Fragments with Short End
484 Homologies. *PLoS ONE* **10**:e0137466.
- 485 10. **Beyer HM, Gonschorek P, Samodelov SL, Meier M, Weber W, Zurbriggen MD.**
486 2015. AQUA Cloning: A Versatile and Simple Enzyme-Free Cloning Approach. *PLoS*
487 *ONE* **10**:e0137652–20.
- 488 11. **García-Nafría J, Watson JF, Greger IH.** 2016. IVA cloning: A single-tube universal
489 cloning system exploiting bacterial In Vivo Assembly. *Sci Rep* **6**:27459.
- 490 12. **Huang F, Spangler JR, Huang AY.** 2017. In vivo cloning of up to 16 kb plasmids in *E.*
491 *coli* is as simple as PCR. *PLoS ONE* **12**:e0183974.
- 492 13. **Gillen JR, Willis DK, Clark AJ.** 1981. Genetic analysis of the RecE pathway of genetic
493 recombination in *Escherichia coli* K-12. *J Bacteriol* **145**:521–532.
- 494 14. **Sain B, Murray NE.** 1980. The hsd (host specificity) genes of *E. coli* K 12. *Mol Gen*
495 *Genet* **180**:35–46.
- 496 15. **Lovett ST.** 2011. The DNA Exonucleases of *Escherichia coli*. *EcoSal Plus* **4**:1–45.

- 497 16. **Demple B, Johnson A, Fung D.** 1986. Exonuclease III and endonuclease IV remove 3'
498 blocks from DNA synthesis primers in H₂O₂-damaged Escherichia coli. *Proc Nat Acad*
499 *Sci* **83**:7731–7735.
- 500 17. **Fijalkowska IJ, Schaaper RM, Jonczyk P.** 2012. DNA replication fidelity in
501 Escherichia coli: a multi-DNA polymerase affair. *FEMS Microbiol Rev* **36**:1105–1121.
- 502 18. **De Lucia P, Cairns J.** 1969. Isolation of an E. coli strain with a mutation affecting DNA
503 polymerase. *Nature* **224**:1164–1166.
- 504 19. **Kornberg A, Baker TA.** 1992. DNA replication.
- 505 20. **Joyce CM, Kelley WS, Grindley ND.** 1982. Nucleotide sequence of the Escherichia
506 coli polA gene and primary structure of DNA polymerase I. *J Biol Chem* **257**:1958–1964.
- 507 21. **Timmis K, Cabello F, Cohen SN.** 1974. Utilization of two distinct modes of replication
508 by a hybrid plasmid constructed in vitro from separate replicons. *Proc Nat Acad Sci*
509 **71**:4556–4560.
- 510 22. **LEHMAN IR, ROUSSOS GG, PRATT EA.** 1962. The deoxyribonucleases of
511 Escherichia coli. II. Purification and properties of a ribonucleic acid-inhibitable
512 endonuclease. *J Biol Chem* **237**:819–828.
- 513 23. **Summers DK, Beton CW, Withers HL.** 1993. Multicopy plasmid instability: the dimer
514 catastrophe hypothesis. *Mol Microbiol* **8**:1031–1038.
- 515 24. **Churchill JJ, Anderson DG, Kowalczykowski SC.** 1999. The RecBC enzyme loads
516 RecA protein onto ssDNA asymmetrically and independently of chi, resulting in
517 constitutive recombination activation. *Genes Dev* **13**:901–911.
- 518 25. **Murray NE.** 2000. Type I restriction systems: sophisticated molecular machines (a
519 legacy of Bertani and Weigle). *Microbiol Mol Biol Rev* **64**:412–434.
- 520 26. **Baba T, Ara T, Hasegawa M, Takai Y, Okumura Y, Baba M, Datsenko KA, Tomita**
521 **M, Wanner BL, Mori H.** 2006. Construction of Escherichia coli K-12 in-frame, single-
522 gene knockout mutants: the Keio collection. *Mol Syst Biol* **2**:2006.0008.
- 523 27. **Datsenko KA, Wanner BL.** 2000. One-step inactivation of chromosomal genes in
524 Escherichia coli K-12 using PCR products. *Proc Nat Acad Sci* **97**:6640–6645.
- 525 28. **Kitagawa R, Ozaki T, Moriya S, Ogawa T.** 1998. Negative control of replication
526 initiation by a novel chromosomal locus exhibiting exceptional affinity for Escherichia
527 coli DnaA protein. *Genes Dev.*
- 528 29. **Chung CT, Niemela SL, Miller RH.** 1989. One-step preparation of competent
529 Escherichia coli: transformation and storage of bacterial cells in the same solution. *Proc*
530 *Nat Acad Sci* **86**:2172–2175.

531 **Figure legends**

532 **Fig. 1 Assays of the iVEC activities**

533 **A.** A scheme of *in vivo* cloning by assembly of two DNA fragments in a cell. DNA
534 fragments containing the *cat* gene and linearized pUC19 DNA have 20 bp homologous
535 overlapping ends (magenta and green). Ampicillin-resistance (Ap^R) and
536 chloramphenicol-resistance (Cm^R) genes are shown in orange and light blue,
537 respectively.

538 **B.** The iVEC activities of various strains are shown as the number of colonies resistant
539 to both ampicillin and chloramphenicol. Averages of three independent experiments
540 (crosses) are shown as circles with standard deviations.

541 **C.** Agarose gel electrophoresis of recombinant plasmids that were purified from the
542 indicated strains. Plasmid DNA of pUC19 prepared from DH5 α was used as a control.

543 **D.** Agarose gel electrophoresis of the plasmid DNA in (C) after digestion with *Bam*HI.

544 **E.** Confirmation of insert DNA by PCR. The insert sequence was amplified by PCR and
545 the length of PCR products was analyzed by agarose gel electrophoresis. pUC19
546 without an insert sequence was used as a negative control.

547 **F.** The iVEC activity of strains with Δ *hsdR* mutation. Statistically significant
548 differences are indicated with asterisks (*p value < 0.05 by Welch's T-test).

549

550 **Fig. 2 Effect of gene mutations on the iVEC activities**

551 **A.** The iVEC activities of the Δ *recA* and Δ *recET* mutant strains are shown as the
552 numbers of colonies resistant to both ampicillin and chloramphenicol. SN1054 was used
553 as the wild-type strain. Averages of three independent experiments (crosses) are shown

554 as circles with standard deviations. n.s.: not significant (p value > 0.05 by Welch's T-
555 test).

556 **B.** The iVEC activities of single-gene deletion mutants for various exonucleases in the
557 Keio collection. Asterisks indicate statistically significant differences (**p value =
558 0.0046 by Welch's T-test).

559 **C.** Transformation efficiency of the $\Delta xthA$ strain. One ng of circular pUC19 DNA was
560 used. Averages of three independent experiments (crosses) are shown as circles with
561 standard deviations. ns indicates that the difference is not statistically significant (p
562 value = 0.77 by Welch's T-test).

563 **D.** A diagram of DNA fragments with blunt ends, 5' overhangs and 3' overhangs. *cat*
564 fragments and linearized pUC19 have 20 bp of homologous sequences at ends (magenta
565 and green).

566 **E.** The iVEC activities by using DNA fragments with blunt ends, 5' overhangs and 3'
567 overhangs. These DNA fragments were introduced into the SN1054 or $\Delta xthA$ mutant.
568 Asterisks indicate statistically significant differences (*p value < 0.05 by Welch's T-
569 test).

570 **F.** The iVEC activities of double gene-deletion mutants: [$\Delta xthA$ and $\Delta recA$] and [$\Delta xthA$
571 and $\Delta recET$]. Asterisks indicate statistically significant difference (**p value = 0.0039
572 by Welch's T-test).

573 **G.** Plasmids assembled in the $\Delta xthA$ mutant strain were analyzed by agarose gel
574 electrophoresis. pUC19 and pUC19-*cat* assembled in the *xthA*⁺ strain (SN1054) were
575 used as a control.

576 **H.** Sequencing of the joint region of the plasmids assembled in the $\Delta xthA$ mutant strain.
577 Eight plasmids of independent single colonies were analyzed.

578

579 **Fig. 3 Involvement of DNA polymerases in the iVEC activity**

580 **A.** The iVEC activity of various strains, which are deletion mutants of non-essential
581 polymerases in the Keio collection, are shown as the numbers of colonies resistant to
582 both ampicillin and chloramphenicol. Averages of six independent experiments
583 (crosses) are shown as circles with standard deviations.

584 **B.** A diagram of functional domains in PolA and PolA1 polymerases. An asterisk
585 indicates the point mutation site (W342 to amber) of *polA1* mutation.

586 **C.** Assembly of the *cat* fragment and linearized pMW119 is shown. Each fragment has
587 20 bp of homologous overlapping sequences shown in green and magenta.

588 **D.** Transformation efficiencies measured by using 1 ng of circular pMW119. Circles
589 indicate averages with standard deviations of three independent experiments (crosses).

590 **E.** The iVEC activity of *polA1* Δ C is shown as the number of colonies resistant to both
591 ampicillin and chloramphenicol after introduction of 0.15 pmol of the *cat* fragment and
592 0.05 pmol of linearized pMW119 into the indicated strains. Averages of six independent
593 experiments (crosses) are shown as circles with standard deviations. Statistically
594 significant differences compared with the parent strain, SN1054, are indicated with
595 asterisks (**p value = 0.0016 or ***p value = 0.00037 by Welch's T-test).

596

597 **Fig. 4 Construction of a strain optimized for iVEC**

598 **A.** Effect of Δ *hsdR* Δ *endA*, and Δ *recA* on the iVEC activities. The iVEC activities are
599 shown as the number of colonies resistant to both ampicillin and chloramphenicol.

600 Averages of three independent experiments (crosses) are shown as circles with standard

601 deviations. Statistically significant differences compared with the MG1655 Δ *hsdR* strain
602 are indicated with asterisks (**p value < 0.01 by Welch's T-test).

603 **B.** Transformation efficiencies measured by using 1 ng of circular pUC19 in each strain.

604 Averages of three independent experiments (cross) are shown as circles with standard
605 deviations. Statistically significant differences compared with the MG1655 Δ *hsdR* strain
606 are indicated with an asterisk (*p value < 0.05 by Welch's T-test).

607 **C.** Agarose gel electrophoresis of recombinant plasmids (pUC19-*cat*). pUC19 was used
608 as a control vector. The monomer and dimer of the plasmids are indicated as arrows.

609

610 **Fig. 5 Performance of the iVEC activity by the optimized strain**

611 **A.** A diagram of the assembly of two DNA fragments with varying lengths of overlaps
612 at the ends.

613 **B.** The iVEC activities by using two DNA fragments with varying lengths of overlaps at
614 the ends are shown as the number of colonies resistant to ampicillin. Averages of three
615 independent experiments (crosses) are shown as circles with standard deviations.

616 Introduction of only linearized pUC19 was also carried out as a negative control.

617 **C.** Proportion of colonies which were resistant to chloramphenicol among the 96
618 ampicillin-resistant colonies in Fig. 5B are shown as the percentage of correct colonies.

619 **D.** A diagram of the assembly of multiple DNA fragments with varying lengths of
620 overlaps at the ends.

621 **E.** The iVEC activities by using multiple DNA fragments with varying lengths of
622 overlaps at the ends are shown as the number of colonies resistant to ampicillin.

623 Averages of three independent experiments (crosses) are shown as circles with standard
624 deviations.

625 **F.** The proportion of colonies that were resistant to antibiotics among the 96 ampicillin-
626 resistant colonies in Fig. 5E are shown as as the percentage of correct colonies correct
627 colonies. Resistance to chloramphenicol and kanamycin was observed for the assembly
628 of three fragments, and resistance to chloramphenicol, kanamycin and tetracycline was
629 observed for the assembly of four and seven fragments of ampicillin-resistant colonies
630 ($n = 96$ except for assembly of the four DNA fragments with 20 bp overlaps, in which n
631 $= 63$).

632 **G.** Agarose gel electrophoresis of the PCR products with or without purification, which
633 were used for the assembly of two fragments.

634 **I.** The iVEC activities by using the PCR products with or without purification are
635 shown as the number of colonies resistant to ampicillin. The PCR products were DNA
636 fragments with 20 bp of overlaps at the ends. Averages of three independent
637 experiments (crosses) are shown as circles with standard deviations.

638

639 **Fig. 6 A model for the mechanism of iVEC**

640

641

642 **Fig. S1 Sequencing of the joint region of the assembled plasmids in SN1187.**

643 Eight plasmids of each construct from independent single colonies were analyzed.

644 Primers used for the sequencing reaction and the percentages of correct sequences are
645 shown.

646 **A.** Joint sequence of plasmids constructed by the assembly of two fragments with 20 bp
647 homologous overlaps.

648 **B.** Joint sequence of plasmids constructed by the assembly of three fragments with 20
649 bp homologous overlaps.

650 **C.** Joint sequence of plasmids constructed by the assembly of four fragments with 20 bp
651 homologous overlaps.

652 **D.** Joint sequence of plasmids constructed by the assembly of seven fragments with 40
653 bp homologous overlaps. A 2 bp region of deletions observed in one of the plasmids is
654 indicated with arrows.

655

656 **Fig. S2 Construction of deletion mutant by two successive homologous**
657 **recombinations.**

658 **A.** Construction of the targeting vector. Linearized pKH5002SB and the upstream and
659 downstream sequences of the target gene were prepared by PCR and assembled in the
660 $\Delta rnhA$ strain. pKH5002SB could be replicated only in RnaseH-deficient strains, due to
661 deletion of the HaeIII fragment in its replication origin.

662 **B.** Deletion of the target gene by two successive homologous recombinations. Since
663 pKH5002SB can be replicated only in RnaseH-deficient strains, the plasmid sequence is
664 not maintained as a plasmid but is maintained in a chromosomally integrated state when
665 the plasmid is introduced into the $rnhA^+$ strains. Cells in which the plasmid sequence is
666 integrated into chromosome are selected by ampicillin. *E. coli* cells harboring the *sacB*
667 gene are not viable on an agar plate containing sucrose, and therefore cells in which the
668 plasmid sequence is dropped out are selected on the sucrose plate.

Figure 1

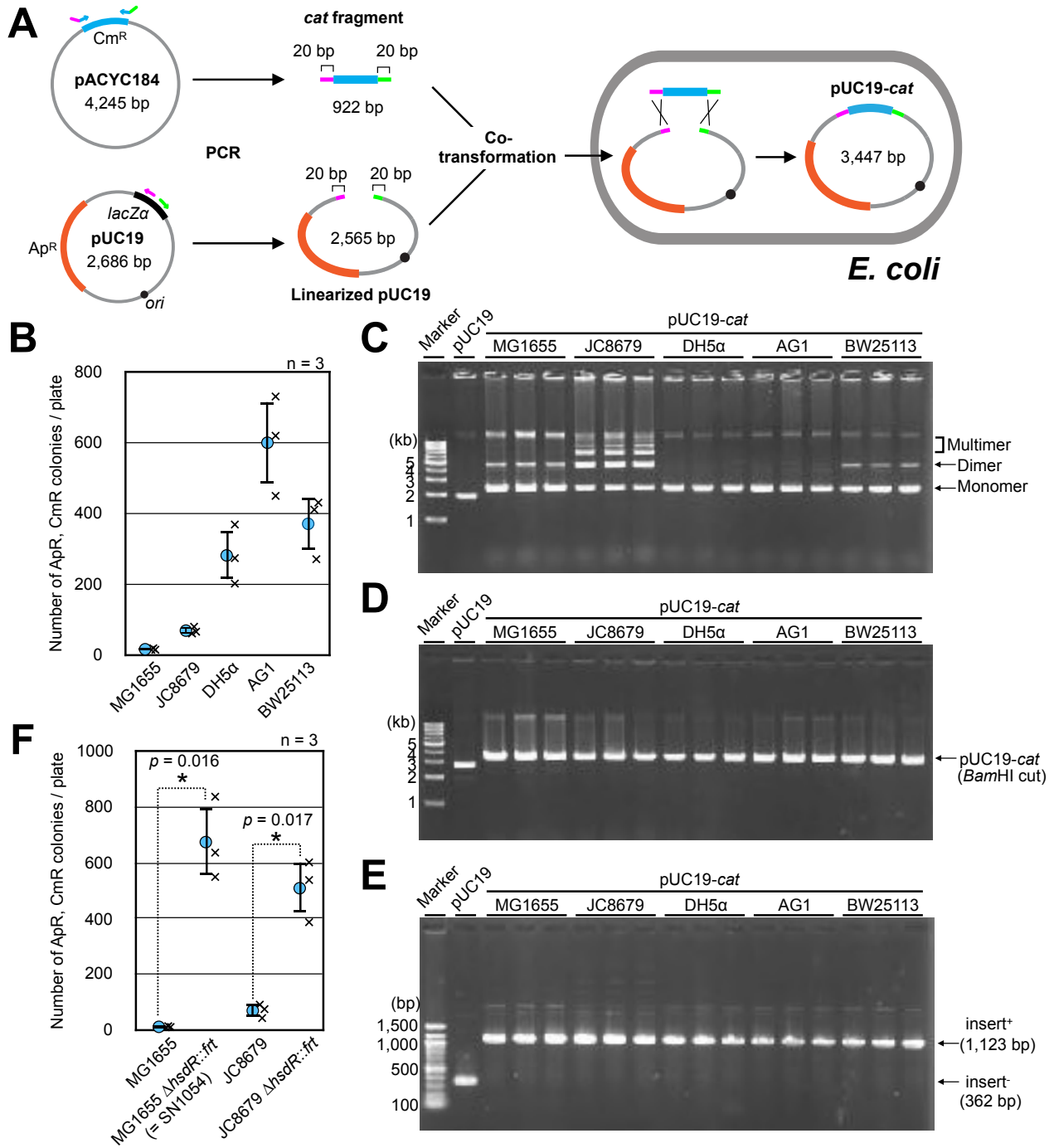


Figure 2

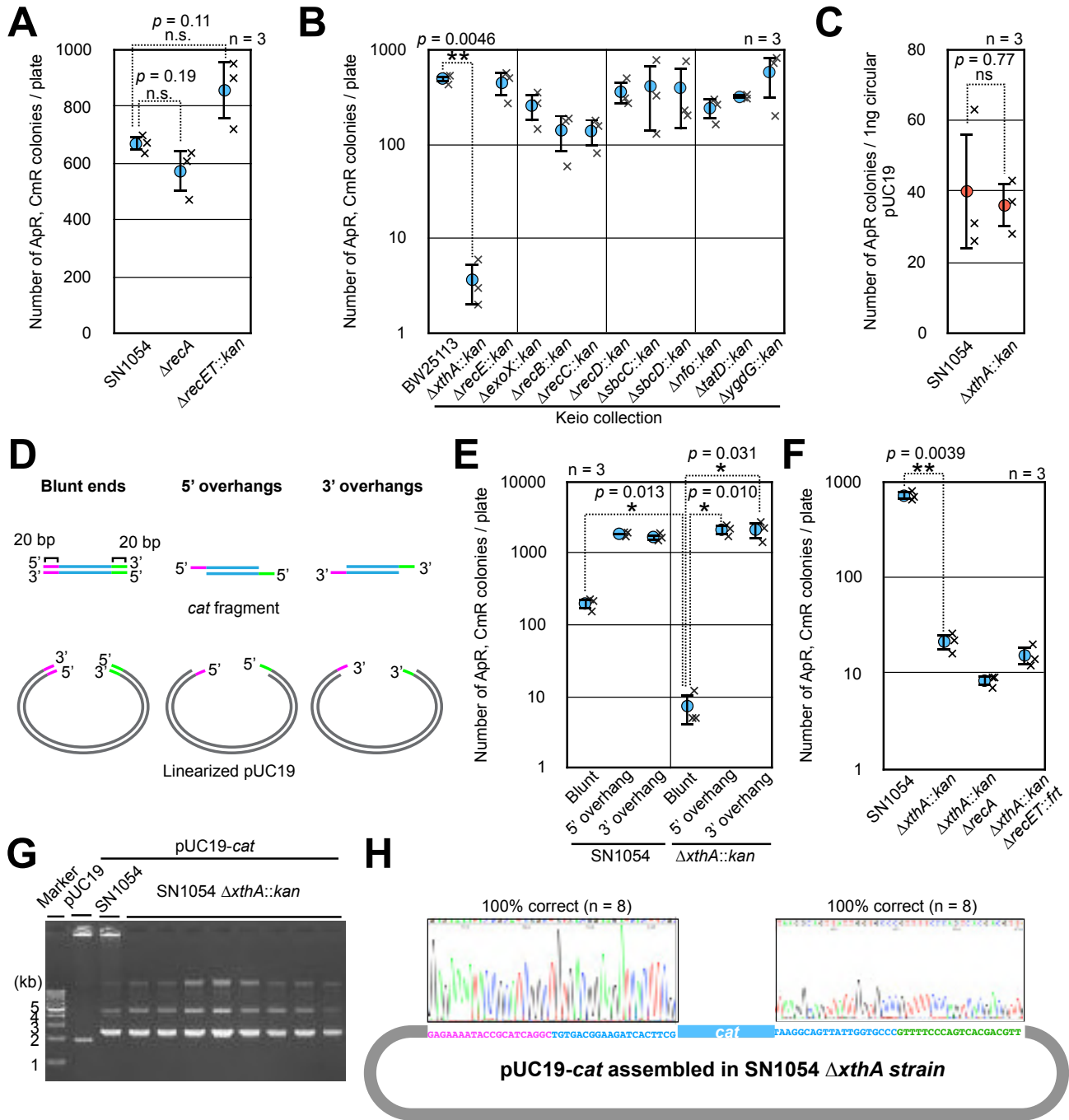


Figure 3

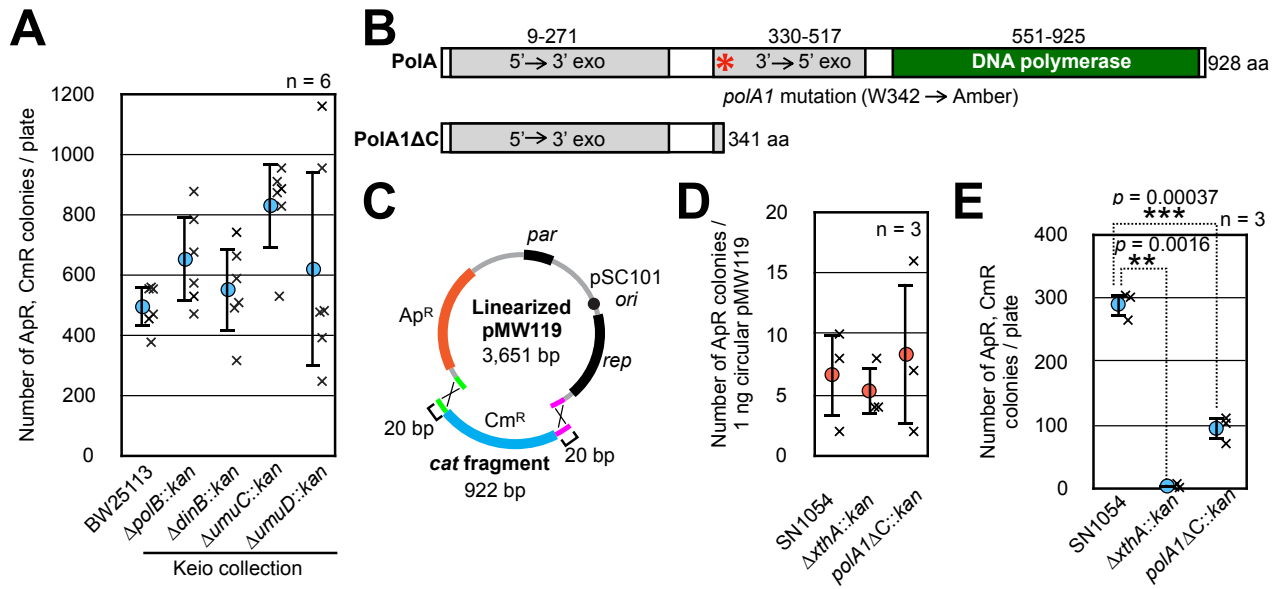


Figure 4

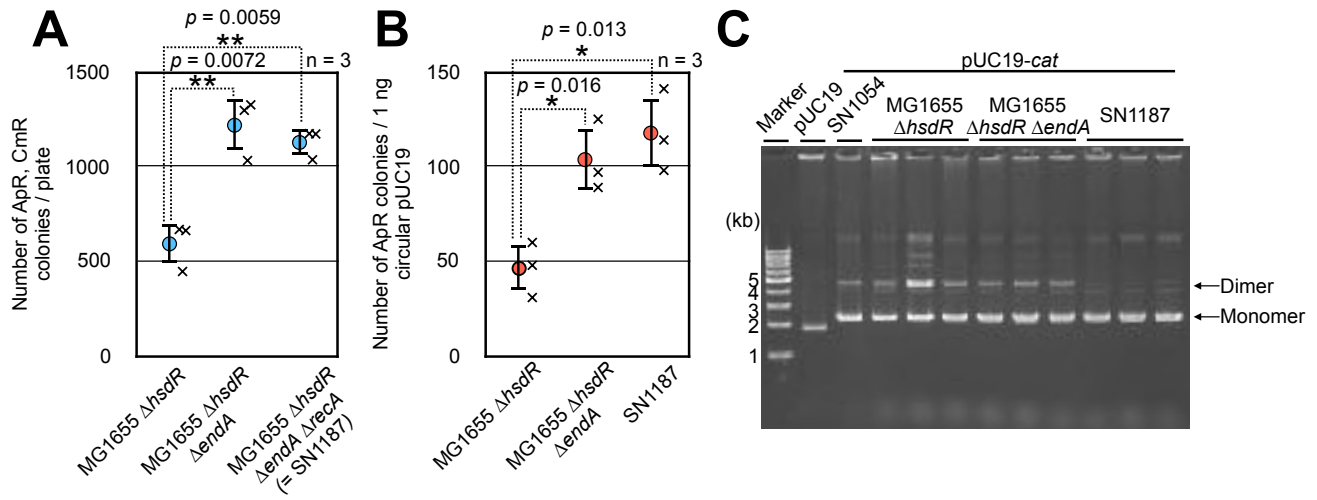


Figure 5

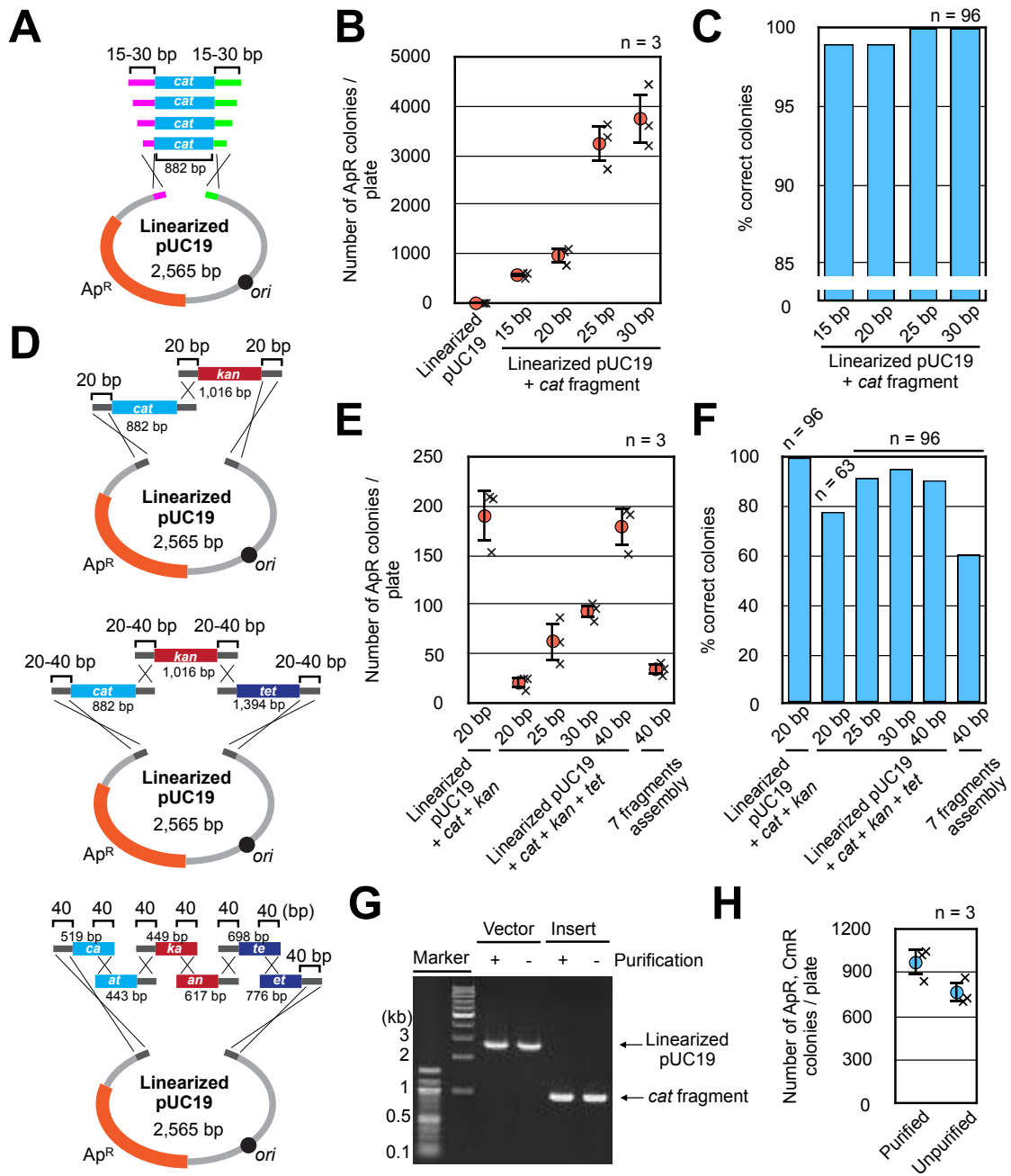


Figure 6

